Quantitative analysis of the nonlinear relationship between neutron or x-ray reflectance and the scattering-length-density profile

Xiao-Lin Zhou
Massachusetts Institute of Technology, 24-215, 77 Massachusetts Avenue, Cambridge, Massachusetts 02139
(Received 27 January 1995; revised manuscript received 20 March 1995)

Understanding the nonlinear relationship between neutron or x-ray reflectance and the scattering-length-density (SLD) profile of a surface film is important for valid and efficient data inversion in reflectivity studies of material films, surfaces, and interfaces. For this reason, a systematic analysis is made of the relationship based on existing reflection theories. Mutual relationships among Parratt's formula (a recurrence relationship in optics for calculating the reflectance of a multilayered film), the nonlinear differential equation, the weighted-superposition approximation (WSA), the distorted-wave Born approximation (DWBA), and the Born approximation (BA) are first explored. Derivations are presented to unify the nonlinear differential equation for the reflectance, the WSA, the DWBA, and the BA under the same Parratt formula. A simplified DWBA formula is also obtained from the WSA and shown to be simpler and more accurate than the regular DWBA formula. Extensive numerical comparisons are carried out to establish well defined ranges of validity for various formulas. In particular, although the BA is useful for analyzing only large-Q data, such as in x-ray studies, the modified BA formula is shown to be very accurate for most free-liquid surfaces. The simplified DWBA is found to be accurate for films on substrates for which an average SLD is well defined. For both free-liquid surfaces and films on substrates in which multiple reflections are weak, the WSA is proven to be accurate over the entire range of Q except some small deviation around the critical edge. Finally, the origin and manifestation of nonlinearity in the reflectance-SLD relationship are discussed quantitatively. The nonlinearity is found to originate from three sources: multiple reflections between interfaces, the nonlinear dependence of the Fresnel reflectance on the SLD, and the dependence of the phase speed of the wave on the SLD. The nonlinearity affects a reflectivity curve in both amplitude and phase and a simple criterion is established for dividing a reflectivity curve into a nonlinear region and a linear region to facilitate data analysis. Results in this analysis may be used as the basis for developing new methods or improving existing methods for model-independent reflectivity data inversion.

PACS number(s): 61.10.Dp, 61.12.Bt, 68.10.−m, 02.50.−r

I. INTRODUCTION

A neutron or x-ray reflectivity curve can be divided into low-, intermediate-, and large-Q regions. In the large-Q region, neutron or x-ray reflectance depends on the scattering-length-density (SLD) profile of the film via a linear Fourier transform relationship represented by the Born (or the kinematic) approximation. In the low- and intermediate-Q regions the relationship becomes complex and nonlinear, as expressed by the discrete Parratt formula or the continuous weighted-superposition approximation (WSA). Data analysis in reflectometry has been a challenging task owing to the complex relationship in the nonlinear regions [1]. As the phase of the reflectance is generally not measured in experiments, the determination of the sample SLD suffers from ambiguity to various degrees depending on the nature of the sample. From an analogy to crystallography [2,3], there has arisen a concern that the sample SLD structure cannot be determined uniquely because the reflectance and the SLD profile are related by a Fourier transform relationship in the large-Q region while the phase is missing in the data. However, a recent work by Zhou and Chen [4] pointed out that the nonlinearity in the low- and intermediate-Q regions following the total reflection plateau might remove some of the ambiguity caused by the lack of phase information. To be more specific, a neutron or x-ray reflectivity curve contains a region of total reflection and a region of nontotal but strong reflection at low and intermediate wave-vector transfer Q. The data in these regions provide useful constraints for determining the correct scattering-length-density (SLD) structure of a surface film. Understanding the nonlinear relationship is important for using reflectivity data in the nonlinear region to remove ambiguity for the determination of the film's SLD structure.

In the study of the relationship of the reflectance and the SLD profile, several approaches have been used to derive analytic formulas for the reflectance. Notably, the standard Green's function approach was used to obtain open-form solutions for the reflectance [5–7]. Depending on how the unknown wave function in an open-form expression is approximated, different approximations are obtained. When the wave function is approximated by the incident wave, the Born approximation (BA) [8–12] results. This approximation essentially assumes that the reflection is weak, so the incident wave is unchanged inside the film. When the wave function of a reference film (say a uniform average film) is used to approximate the unknown wave function in the actual film, a more consistent approximation, called the distorted-wave Born ap-

proximation (DWBA) [13–16], is obtained. A generalized form of the DWBA can be found in a paper by Sears [17]. These approximations have a limited range of validity. Other approximations with different or increased ranges of validity include the small curvature approximation (SCA) [6] and the modified WKB approximation (MWKB) [7]. A recent development in the reflection theory is the weighted-superposition approximation (WSA) by Zhou and He [18]. This approximation was simple in form, was shown to be valid over the entire range of Q, and was more accurate than all existing approximations.

To gain insight into the physical contents of these analytic formulas for the reflectance as a function of the SLD profile, a systematic study is needed to compare them with each other and link them with the exact Parratt recurrence formula. As Parratt's formula is an exact solution of the wave equation [19,20] for a stack of N discrete, uniform layers, the WSA, the DWBA, and the BA should all be derivable from Parratt's formula in the continuous limit. The BA should also be derivable from the WSA because the BA is the linear limit of the nonlinear WSA. The exact differential equation for the reflectance inside a surface film should also be derivable from Parratt's formula in the continuous limit, as both are exact solutions of the wave equation. We will make these derivations in this paper to unify reflection theories. As data analysis demands an accurate understanding of the ranges of validity of the approximate formulas used, we will make a numerical evaluation of these formulas for a variety of practical SLD profiles and determine which formula is accurate for what profiles. To achieve an unambiguous understanding of the nonlinear region of a reflectivity curve, we will analyze Parratt's formula, the WSA, the DWBA, and the BA comparatively to determine the origin and manifestation of nonlinearity and how it affects the reflectivity data in the small and intermediate Q regions.

In this paper, the mutual relationships among Parratt's formula, the WSA, the DWBA, the BA, and the differential equation for the reflectance, and their numerical comparisons will be discussed in Sec. II. The nonlinearity analysis will be presented in Sec. III. Note that in Sec. II, the WSA, the DWBA, and the BA will each be derived through three different methods, showing their roots of origination, and a different, simplified DWBA formula will be derived. The discussion in this paper applies to both x-ray and neutron grazing-angle reflection, since both the x ray and the neutron obey a wave equation of the same form [20].

II. ANALYSIS OF EXISTING REFLECTION THEORIES

We discuss the mutual relationships among Parratt's formula, the differential equation for the reflectance, the WSA, the DWBA, the simplified DWBA, the BA, and the modified BA, and their ranges of validity. Since Parratt's formula is an exact solution of the wave equation, we will show how to use it to derive the differential equation and all other approximate formulas in the continuous limit. We also show how to derive the BA from the WSA in the linear limit and how to obtain the BA for reflection from the general theory of scattering. The derivation of a simplified DWBA will also be presented.

A. Nonlinear differential equation for reflectance

The goal is to derive a nonlinear differential equation for the reflectance from the discrete Parratt formula by taking the continuous limit. For a stack of N layers each having a constant SLD and a given thickness, the reflectance can be calculated according to Parratt's recurrence formula [19]

$$r_n=\frac{R_{n+1}+r_{n+1}\exp(2ik_{n+1}\Delta z_{n+1})}{1+R_{n+1}r_{n+1}\exp(2ik_{n+1}\Delta z_{n+1})}\ , \tag{1}$$

where R_{n+1} is the Fresnel reflectance of the interface between layer n and layer $n+1$, Δz_{n+1} is the thickness of layer $n+1$, k_{n+1} is the value of k inside layer $n+1$ related to the SLD ρ_{n+1} by $k_{n+1}=(k_0^2-4\pi\rho_{n+1})^{1/2}$, r_n is the reflectance of the entire region beneath the interface at z_n, and r_{n+1} the reflectance of the region beneath the interface at z_{n+1}.

Let us assume that a surface film profile is divided into N layers with each layer having the same thickness Δz. It can be shown that the Fresnel reflectance of the interface between the layer $(z-\Delta z,z)$ and the layer $(z,z+\Delta z)$ is proportional to the first power of Δz. Expanding the exponential terms in Eq. (1) and keeping only the first-order terms, we obtain

$$r_n=\frac{r_{n+1}+\left[2ik_{n+1}r_{n+1}+\dfrac{R_{n+1}}{\Delta z}\right]\Delta z}{1+r_{n+1}\left[\dfrac{R_{n+1}}{\Delta z}\right]\Delta z}\ . \tag{2}$$

Noting the following relations,

$$\lim_{\Delta z\to 0}\left[\frac{R_{n+1}}{\Delta z}\right]=-\frac{k'}{2k}\ , \tag{3}$$

$$\lim_{\Delta z\to 0}\frac{r_{n+1}-r_n}{\Delta z}=r'\ , \tag{4}$$

we take the limit that Δz tends to zero in Eq. (2) to reach

$$r'+2ikr+\frac{k'}{2k}(r^2-1)=0\ , \tag{5}$$

which is identical to the one derived in [21], although a different approach was used there. Equation (5) is an exact differential equation equivalent to Parratt's formula and is a nonlinear equation because it contains r^2. If we consider the dependence of r on the SLD ρ, it is clear from Eq. (5) that there are three sources of nonlinearity in the dependence: the phase coefficient $2ik$, the Fresnel reflectance coefficient $k'/2k$, and the r^2 term due to multiple reflections. We will discuss the origin of nonlinearity in more detail in Sec. III.

B. Weighted-superposition approximation (WSA)

The WSA was derived in detail in [18] based on the principle of superposition. For convenience of discussion, we describe the coordinate system and notations by a brief derivation of the WSA. As shown in Fig. 1, a coordinate system is set up such that a surface film occupies the region $(-d,0)$, the substrate (or bulk), the region $(0,\infty)$, and the incident space $(-\infty,-d)$. A plane wave is incident on the sample from the free-space region. The wave has a wavelength λ and makes a grazing angle of incidence θ with the sample surface. The projection of the wave vector of the wave in the direction perpendicular to the sample surface is $k_0=2\pi/\lambda\sin\theta$. The sample SLD profile $\rho(z)$ is divided into an infinite number of histogramlike small differential SLD steps distributed along the depth direction z. A simple elemental Fresnel reflection is assumed to occur at each of the steps. The weighted sum of all the elemental Fresnel-reflected wavelets is equal to the reflection from the entire sample. First, the elemental Fresnel reflection at the differential step at z_n is given by

$$R_n=\frac{k(z_n-\Delta z/2)-k(z_n+\Delta z/2)}{k(z_n-\Delta z/2)+k(z_n+\Delta z/2)}\ , \tag{6}$$

which satisfies

$$\lim_{\Delta z\to dz} R_n=\frac{\pi(d\rho/dz)}{k^2}dz\ . \tag{7}$$

The accumulated phase along both the incident path and the reflection path by the wave reflected at z_n is given by

$$W(z_n)=\exp\left[2i\int_{-d}^{z_n}k(z)dz\right]\ . \tag{8}$$

Summing the product of Eq. (7) and Eq. (8) over "n" under the limit of "n" tending to infinity, we get

$$r=\pi\int_{-d}^{\infty}dz\frac{d\rho/dz}{k^2}\exp\left[2i\int_{-d}^{z}k(z)dz\right]\ , \tag{9}$$

which is the weighted-superposition approximation (WSA) presented by Eq. (9) in [18].

1. Derivation of the WSA from Parratt's formula

We show here that the WSA can be derived directly from Parratt's formula Eq. (1). As measured reflectivity spans a range from total reflection down to 10^{-6}, 10^{-7}, or even lower, the second term in the denominator of Eq. (1) is much smaller than the first term, which is unity, for most part of a reflectivity curve. This is true even if r_{n+1} and R_{n+1} are respectively as large as 0.2 in magnitude. Thus,

$$r_n\approx R_{n+1}+r_{n+1}\exp(2ik_{n+1}\Delta z_{n+1}) \tag{10}$$

is a very accurate approximation of Eq. (1). The recursion in Eq. (10) can be carried out to obtain

$$r_0\approx\sum_{p=1}^{N+1}R_p\exp\left[2i\sum_{q=1}^{p-1}k_q\Delta z_q\right]\ , \tag{11}$$

where r_0 is the reflectance of the entire film and R_p is the Fresnel reflectance of the interface between layer $p-1$ and layer p given by

$$R_p=\frac{k_{p-1}-k_p}{k_{p-1}+k_p}=4\pi\left[\frac{\rho_p-\rho_{p-1}}{\Delta z_p}\right]\frac{\Delta z_p}{(k_{p-1}+k_p)^2}\ . \tag{12}$$

Combining Eq. (11) with Eq. (12) under the limit that Δz_p and Δz_q vanish and N approaches infinity, we obtain

$$r=\pi\int_{-d}^{\infty}dz\frac{d\rho/dz}{k^2}\exp\left[2i\int_{-d}^{z}k(z)dz\right]\ , \tag{13}$$

which is identical to Eq. (9), derived through a different method.

2. Derivation of the WSA from the differential equation (5)

If the square term in the parenthesis in Eq. (5) is negligible compared to unity, say, the magnitude of r is less than 0.2, then Eq. (5) reduces to a linear equation

$$r'+2ikr-\frac{k'}{2k}=0\ , \tag{14}$$

a solution of which is

$$r(z)=-\exp\left[-2i\int_{-d}^{z}k(z)dz\right]\times\int_{z}^{\infty}dz\frac{k'}{2k}\exp\left[2i\int_{-d}^{z}k(z)dz\right]\ . \tag{15}$$

The reflectance of the surface film is equal to $r(z)$ evaluated at the air-film interface $z=-d$:

$$r\equiv r(-d)=\pi\int_{-d}^{\infty}dz\frac{d\rho/dz}{k^2}\exp\left[2i\int_{-d}^{z}k(z)dz\right]\ , \tag{16}$$

which is identical to the WSA in Eq. (9).

In the derivation, it is obvious that the WSA omits the multiple reflection effect by neglecting r^2. However, it has completely included the nonlinear dependence of r on $\rho(z)$ through the phase coefficient $2ik(z)$ and the Fresnel reflectance term $k'/2k$. Fortunately, multiple reflections are negligible for most parts of a reflectivity curve because the maximum magnitude of r^2 in Eq. (5) is of the same order as of the measured reflectivity $|r|^2$. As a result, the relative error introduced in the WSA is of the order of $|r|^2$ and is negligible for reflectivities less than 0.1. Larger errors only affect the region from the critical edge down to 0.1 in reflectivity, and we know that this re-

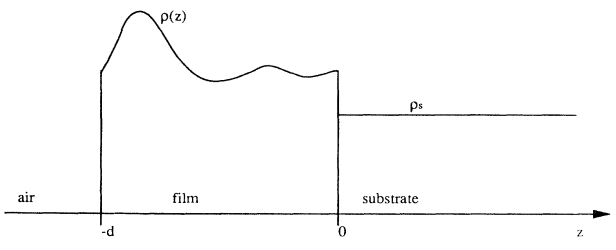

FIG. 1. Illustration of the three space regions: the incident space $z<-d$, the film $-d<z<0$, and the substrate $z>0$. The SLD of the air region, the film, and the substrate is, respectively, 0, $\rho(z)$, and ρ_s.

gion is very narrow in a typical reflectivity curve. In the total reflection plateau, the reflectivity is dominated by the Fresnel reflectivity of a major interface in the film and the wave is evanescent, so that the effect of multiple reflections is again not very significant. As a result, the total reflection plateau can be well represented by the WSA, as shown by the calculations in [18].

C. Distorted-wave Born approximation (DWBA)

The spirit of the DWBA was given in [13] and a simple derivation of the DWBA for the reflectance can be found in [14]. The essence of the DWBA is to treat a surface film as the sum of a known reference film and a small derivation from the reference film. Thus reflection from the reference film is dominant and contribution from the deviation should be comparatively small. Before we show that the DWBA can be derived from Parratt's formula, we define the notations in the DWBA through a traditional derivation of the DWBA as given in [14]. As shown in Fig. 2, the simplest reference film is a uniform film with a constant SLD $\bar{\rho}$ and thickness d situated on top of the same substrate with the SLD $=\rho_s$. The SLD of the surface film is related to the reference film SLD, $\bar{\rho}$, by

$$\rho=\bar{\rho}+\Delta\rho \ , \tag{17}$$

where $\Delta\rho$ is the deviation of the surface film SLD from the reference film SLD, and its average in $(-d,0)$ equals zero. The reflectance of the reference film plus the substrate $\bar{R}$ can easily be calculated by solving the one-dimensional wave equation $U''(z)+\bar{k}^2U(z)=0$ with $\bar{k}^2=k_0^2-4\pi\bar{\rho}$, and matching the continuity boundary conditions at the air-film and film-substrate interfaces. The reflectance of the actual film should be calculated from the wave equation $U''(z)+k^2U(z)=0$, which can be written as

$$U''(z)+\bar{k}^2U(z)=(\bar{k}^2-k^2)U(z) \ . \tag{18}$$

Regarding the right-hand side of this equation as a source term and using the Green's function approach, we obtain an exact solution of Eq. (18) as [7]

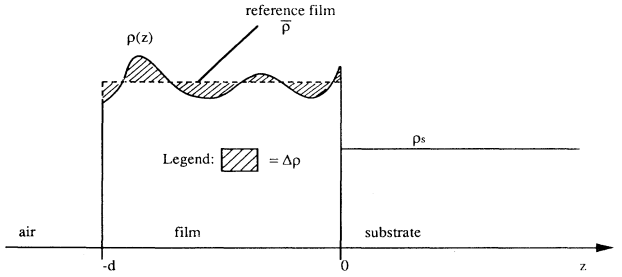

FIG. 2. Geometry showing that a reflecting system can be treated as the sum of a reference film system plus a deviation. The reference system, as indicated by the dashed line, consists of the incident space, a constant film with SLD $\bar{\rho}$, and the same substrate with SLD ρ_s. The deviation $\Delta\rho$ and the reference SLD $\bar{\rho}$ add up to the total SLD $\rho(z)$.

$$r=\bar{R}e^{-2ik_0d}+A\int_{-d}^{0}dz'(\bar{k}^2-k^2)U(z') \times(e^{i\bar{k}z'}+R_re^{-i\bar{k}z'}) \ , \tag{19}$$

with

$$\bar{R}=C(-R_l+R_re^{2i\bar{k}d}) \ , \tag{20}$$

$$A=-\frac{iC}{2\bar{k}}T_-e^{i(\bar{k}-k_0)d} \ , \tag{21}$$

$$C=\frac{1}{1-R_lR_re^{2i\bar{k}d}} \ , \tag{22}$$

$$T_+=\frac{2k_0}{k_0+\bar{k}}, \quad T_-=\frac{2\bar{k}}{k_0+\bar{k}} \ ,$$

$$R_l=\frac{\bar{k}-k_0}{\bar{k}+k_0}, \quad R_r=\frac{\bar{k}-k_s}{\bar{k}+k_s} \ , \tag{23}$$

where R_l and R_r are the Fresnel reflectances of the film-air interface and the film-substrate interface, respectively. The quantities k_0, $\bar{k}$, and k_s are the perpendicular component of the wave vector in air, the reference film, and the substrate (or bulk), respectively.

Under the DWBA, the wave function $U(z)$ in Eq. (19) is approximated by the solution of $U''(z)+\bar{k}^2U(z)=0$, which is

$$U(z)\approx T_+Ce^{i(\bar{k}-k_0)d}(e^{i\bar{k}z}+R_re^{-i\bar{k}z}) \ . \tag{24}$$

Substituting Eq. (24) into Eq. (19) leads to

$$r=e^{-2ik_0d}\left\{\bar{R}+\frac{2\pi}{i\bar{k}}T_+T_-C^2 \times[\Delta\tilde{\rho}(2\bar{k})+R_r^2e^{4i\bar{k}d}\Delta\tilde{\rho}(-2\bar{k})]\right\} , \tag{25}$$

which is the DWBA result given by Eq. (8) in Ref. [14]. Here $\Delta\tilde{\rho}$ denotes the Fourier transform of the deviation $\Delta\rho$. Note that the constant phase factor e^{-2ik_0d} is due to the location of the origin $z=0$ at the film-substrate interface and can be omitted without affecting the reflectivity.

1. *Derivation of the DWBA from Parratt's formula*

Here we show how to derive the DWBA from Parratt's formula. For a film that is a small deviation from a reference film, we first approximate the air-film interface and the film-substrate interface of the film by those of the reference film. The air-film interface has two sides, $z=-d^-$ in air and $z=-d^+$ in the film. The reflectance r of the entire system is the value of $r(z)$ evaluated at $z=-d^-$; that is, $r(-d^-)$. According to Parratt's formula Eq. (1), this reflectance is related to the reflectance inside the film $r(-d^+)$ by

$$r\equiv r(-d^-)=\frac{-R_l+r(-d^+)}{1-R_lr(-d^+)} \ . \tag{26}$$

Note that $-R_l$ is equal to the Fresnel reflectance of the air-film interface of the reference film for a wave incident

from air. Now we calculate $r(-d^+)$ by integrating Eq. (5). Formal integration leads to

$$r(z)=-\exp\left[-2i\int_{-d}^{z}k(z)dz\right]\times\int_{z}^{\infty}dz\frac{k'}{2k}(1-r^2)\exp\left[2i\int_{-d}^{z}k(z)dz\right], \quad (27)$$

thus,

$$r(-d^+)=\pi\int_{-d^+}^{\infty}dz\frac{\rho'}{k^2}(1-r^2)\exp\left[2i\int_{-d}^{z}k(z)dz\right]. \quad (28)$$

Equation (28) is exact but "$r(z)$" inside the film is unknown. We now find a way to calculate it approximately. For the reference film, we know that

$$\bar{r}(z)=R_r\exp(-2i\bar{k}z). \quad (29)$$

Applying Eq. (28) to the reference film and comparing it with Eq. (29) at $z=-d^+$, we get

$$\bar{r}(-d^+)=R_r\exp(2i\bar{k}d)=\pi\int_{-d^+}^{\infty}dz\frac{\bar{\rho}'}{\bar{k}^2}[1-\bar{r}^2]\exp\left[2i\int_{-d}^{z}\bar{k}\,dz\right], \quad (30)$$

where the quantities with an overbar pertain to the reference film. Note that, although $\bar{\rho}$ is a constant inside the film, it contains discontinuity at $z=0$ so that $(\bar{\rho})'$ is nonvanishing. Substituting Eq. (17) into the right-hand side of Eq. (28), approximating $r(z)$ by $\bar{r}(z)$ given in Eq. (29), approximating $k(z)$ by $\bar{k}$, and using Eq. (30), we have

$$r(-d^+)\approx R_r\exp(2i\bar{k}d)+\pi\int_{-d^+}^{\infty}dz\frac{(\Delta\rho)'}{k^2}[1-R_r^2\exp(-4i\bar{k}z)]\times\exp\left[2i\int_{-d}^{z}\bar{k}(z)dz\right]. \quad (31)$$

Carrying out integration by parts in the second term and noting that $\Delta\rho$ vanishes at $z=-d$ and $z=0$, we obtain

$$r(-d^+)=R_r\exp(2i\bar{k}d)+Y, \quad (32)$$

$$Y\equiv-\frac{\pi}{\bar{k}^2}\int_{-d^+}^{\infty}dz\,\Delta\rho\frac{d}{dz}\times\{[1-R_r^2\exp(-4i\bar{k}z)]\exp[2i\bar{k}(z+d)]\}. \quad (33)$$

Substituting Eq. (32) into Eq. (26), regarding Y as a small term, and expanding it to first order of Y, we obtain

$$r(-d^-)\approx\frac{-R_l+R_r\exp(2i\bar{k}d)}{1-R_lR_r\exp(2i\bar{k}d)}+\frac{Y(1-R_l^2)}{[1-R_lR_r\exp(2i\bar{k}d)]^2}. \quad (34)$$

The value of Y can be evaluated as

$$Y=\frac{2\pi}{i\bar{k}}\int_{-d}^{\infty}dz\,\Delta\rho\{\exp[2i\bar{k}(z+d)]+e^{4i\bar{k}d}R_r^2\exp[-2i\bar{k}(z+d)]\}=\frac{2\pi}{i\bar{k}}[\Delta\tilde{\rho}(2\bar{k})+R_r^2e^{4i\bar{k}d}\Delta\tilde{\rho}(-2\bar{k})]. \quad (35)$$

Using Eq. (20), we get

$$r=\bar{R}+\frac{2\pi}{i\bar{k}}\frac{(1-R_l^2)}{[1-R_lR_r\exp(2i\bar{k}d)]^2}\times[\Delta\tilde{\rho}(2\bar{k})+R_r^2e^{4i\bar{k}d}\Delta\tilde{\rho}(-2\bar{k})], \quad (36)$$

which can be easily shown to be equal to Eq. (25) derived from the Green's function approach, except for an nonessential phase constant due to a shift by d of the origin of the coordinate system to the air-film interface compared to that in Fig. 2.

2. *Derivation of a simplified DWBA from the WSA*

In this section, we derive a simplified DWBA from the WSA. Applying the WSA Eq. (9) to the reference film with SLD $\bar{\rho}$ on top of a substrate of SLD ρ_s, we get

$$\bar{R}=\pi\int_{-d}^{\infty}dz\frac{d\bar{\rho}/dz}{\bar{k}^2}\exp\left[2i\int_{-d}^{z}\bar{k}(z)dz\right]. \quad (37)$$

Substituting Eq. (17) into Eq. (9), we obtain

$$r=\pi\int_{-d}^{\infty}dz\frac{d\bar{\rho}/dz}{k^2}\exp\left[2i\int_{-d}^{z}k(z)dz\right]+\pi\int_{-d}^{\infty}dz\frac{d(\Delta\rho)/dz}{k^2}\exp\left[2i\int_{-d}^{z}k(z)dz\right]. \quad (38)$$

Approximating $k(z)$ by $\bar{k}$ and using Eq. (37), we obtain

$$r\approx\bar{R}+\pi\int_{-d}^{\infty}dz\frac{d(\Delta\rho)/dz}{\bar{k}^2}e^{2i\bar{k}(z+d)}. \quad (39)$$

Calculating the integral by integration by parts, we obtain

$$r\approx\bar{R}+\frac{2\pi}{i\bar{k}}\int_{-d}^{\infty}dz\,\Delta\rho\exp[2i\bar{k}(z+d)]=\bar{R}+\frac{2\pi}{i\bar{k}}\Delta\tilde{\rho}(2\bar{k}). \quad (40)$$

Comparing Eq. (40) with the DWBA formula Eq. (25), we find that Eq. (40) is equal to the DWBA result Eq. (25) if terms proportional to R_r^2 and R_rR_l are ignored compared with unity, in accordance with the spirit of the WSA. Calculations in Sec. E will show that Eq. (40) is as accurate as Eq. (25) for free-liquid surfaces that are small deviations from the reference film, but is more accurate than Eq. (25) for profiles that significantly deviate from the reference film.

D. The Born approximation (BA)

We will show that the BA can be derived directly from Parratt's formula. We will also show that the BA is the linear limit of the WSA. Before making such derivations,

we first demonstrate that the BA for specular reflection from a surface film can be obtained by specializing the general theory of scattering under the weak scattering approximation to the one-dimensional surface film. Here we only discuss neutron wave reflection because x-ray reflection can be obtained analogously.

Reflection of a wave from a stratified medium is a special case of wave scattering from an arbitrary three-dimensional (3D) scatterer. If the total 3D wave function is denoted as $\psi(\bar{r})$ and the 3D scattered wave function as $\psi_s(\bar{r})$, then they are related to the incident wave function $\psi_i(\bar{r})$ by $\psi(\bar{r})=\psi_i(\bar{r})+\psi_s(\bar{r})$. The scattered wave satisfies the following exact integral equation [20]:

$$\psi_s(\bar{r})=-\int d\nu' \frac{e^{iqR}}{R}\rho(\bar{r}')\psi(\bar{r}') , \tag{41}$$

where dv' is an elemental volume in the scatterer, $R=|\bar{r}-\bar{r}'|$ is the distance from the source point $\bar{r}'$ to the field point $\bar{r}$, and q is the magnitude of the 3D free-space wave vector. Substituting $\psi(\bar{r})=\psi_i(\bar{r})+\psi_s(\bar{r})$ into Eq. (41), we get

$$\psi_s(\bar{r})=-\int d\nu' \frac{e^{iqR}}{R}\rho(\bar{r}')\psi_i(\bar{r}') - \int d\nu' \frac{e^{iqR}}{R}\rho(\bar{r}')\psi_s(\bar{r}') . \tag{42}$$

The first term is the first Born approximation in three dimensions and is obviously due to the direct illumination of $\rho(\bar{r}')$ by the incident wave $\psi_i(\bar{r}')$. The second term is the multiple scattering effect because the source term $\rho(\bar{r}')\psi_s(\bar{r}')$ is due to the illumination of the SLD profile by the scattered wave $\psi_s(\bar{r})$, which itself arises from $\rho(\bar{r}')$. Omitting multiple scatterings,

$$\psi_s(\bar{r})\approx-\int d\nu' \frac{e^{iqR}}{R}\rho(\bar{r}')\psi_i(\bar{r}') . \tag{43}$$

This is valid only when scattering is dominated by single scatterings, which means scattering is very weak. For instance, if the single scattering amplitude is 10^{-2} times the incident wave, double scattering is 10^{-4} and is negligible. However, if the single scattering amplitude is 0.5 times the incident wave, double scattering is 0.25 and triple scattering is 0.125, and both are not negligible. It is important to know that all multiple scatterings are omitted in obtaining Eq. (43) and only single scatterings are included.

For a plane wave $\psi_i(\bar{r})=e^{iq\hat{i}\cdot\bar{r}}$ incident on a stratified medium, $\rho(\bar{r}')=\rho(z')$, we have

$$\psi_S(\bar{r})=-\int d\nu' \frac{e^{iqR}}{R}\rho(z')e^{iq\hat{i}\cdot\bar{r}'} . \tag{44}$$

In the specular direction, the outgoing scattered wave vector makes the same angle θ with the xy plane as does the incident wave vector, and the scattering plane coincides with the yz plane. As shown in Fig. 3, the distance R can be approximated in the far field as

$$R\approx R_0-y'\cos\theta+\frac{x'^2+y'^2\sin^2\theta}{2R_0} , \tag{45}$$

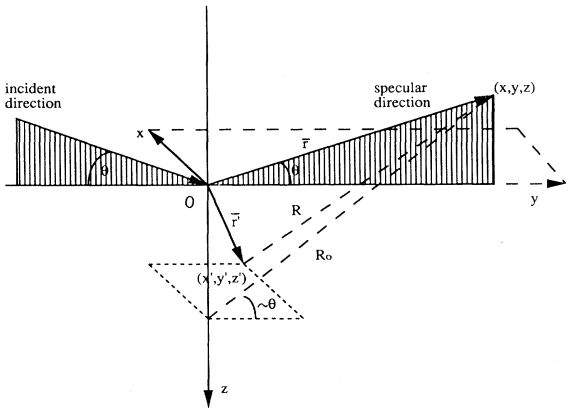

FIG. 3. Geometry showing the field point $\bar{r}$ relative to the source point $\bar{r}'$. The stratification plane coincides with the xy plane and the scattered wave direction makes the same angle θ with the xy plane as the incident wave does. The distance R between the source point and the field point can be approximated by Eq. (45) when $r' \ll r$ in the far field.

and $R_0\approx r+z'\sin\theta$. Replacing R by R_0 in the denominator of Eq. (44) and by Eq. (45) in the numerator, integrating with respect to x' and y' over $(-\infty,\infty)$, one obtains

$$\psi_S(\bar{r})=-\frac{4\pi i}{Q}e^{iqr}\int dz'\rho(z')e^{iQz'} , \tag{46}$$

where $Q=4\pi\sin\theta/\lambda$. The reflection coefficient of the surface is the amplitude of the scattered plane wave e^{iqr}, so the BA for the reflectance is [8–12]

$$r=\frac{-4\pi i}{Q}\int\rho(z')e^{iQz'}dz'=\frac{4\pi}{Q^2}\int\frac{d\rho(z')}{dz'}e^{iQz'}dz' . \tag{47}$$

1. *Derivation of the BA from Parratt's formula*

Under the Born approximation as discussed above, reflection is assumed to be weak in the film, implying that R_{n+1} and r_{n+1} in Eq. (1) are much less than unity. In addition, a reflected wavelet travels in free space without phase drag, i.e., k can be approximated by the free-space value k_0. According to Eq. (1), we have

$$r_n\approx R_{n+1}+r_{n+1}\exp(2ik_0\Delta z_{n+1}) . \tag{48}$$

Carrying out the recurrence, we obtain

$$r_0\approx\sum_{p=1}^{N+1}R_p\exp\left[2ik_0\sum_{q=1}^{p-1}\Delta z_q\right] , \tag{49}$$

where Fresnel reflectance R_p of the interface between layer $p-1$ and layer p can be approximated as

$$R_p=\frac{k_{p-1}-k_p}{k_{p-1}+k_p}\approx\frac{\pi(\rho_p-\rho_{p-1})}{k_0^2} . \tag{50}$$

Thus

$$r_0\approx\frac{\pi}{k_0^2}\sum_{p=1}^{N+1}(\rho_p-\rho_{p-1})\exp\left[2ik_0\sum_{q=1}^{p-1}\Delta z_q\right] . \tag{51}$$

Taking the limit that N approaches infinity and Δz_q ap-

proaches zero, we obtain

$$r=\frac{\pi}{k_0^2}\int_{-d}^{\infty}dz\frac{d\rho}{dz}e^{2ik_0z}=\frac{4\pi}{Q^2}\int_{-d}^{\infty}dz\frac{d\rho}{dz}e^{iQz}\ , \tag{52}$$

which is the Born approximation formula for the reflectance.

2. *Derivation of the BA from the WSA*

At large wave-vector transfer Q, $k_0^2 \gg 4\pi\rho$, so $k\approx k_0$. The integral in the exponential term in the weighted-superposition approximation Eq. (9) can be approximated as $2ik_0(z+d)$ and the amplitude term becomes π/k_0^2. Thus, the WSA can be reduced to

$$r=e^{2ik_0d}\frac{\pi}{k_0^2}\int_{-d}^{\infty}dz\frac{d\rho}{dz}e^{2ik_0z}\ . \tag{53}$$

The constant phase factor $\exp(2ik_0d)$ comes about because the WSA takes $z=-d$ as the reference point for zero phase. If we translate the coordinate system so that the air-film interface location is the reference point for zero phase, one has

$$r=\frac{\pi}{k_0^2}\int_{-d}^{\infty}dz\frac{d\rho}{dz}e^{2ik_0z}=\frac{4\pi}{Q^2}\int_{-d}^{\infty}dz\frac{d\rho}{dz}e^{iQz}\ , \tag{54}$$

which is identical to the BA in Eq. (47).

The Born approximation as given by Eq. (47), Eq. (52), or Eq. (54) can be modified to apply to liquid surfaces with an improved accuracy. We know that the reflectance of a sharp surface of a uniform bulk liquid with SLD ρ_b is equal to the Fresnel reflectance R_b. As the slope of the SLD of such a surface is a δ function located at the surface, Eq. (54) gives a different result. By forcing this result to equal R_b, we get

$$R_b=\frac{4\pi\rho_b}{Q^2}\ . \tag{55}$$

Dividing Eq. (55) into Eq. (54), we obtain the modified Born approximation

$$r=\frac{R_b}{\rho_b}\int_{-\infty}^{\infty}dz\frac{d\rho}{dz}e^{iQz}\ , \tag{56}$$

which has been widely used by many authors [8–12].

E. Numerical evaluation of the ranges of validity

The analytical derivations in the above have revealed the origins of errors introduced in reaching various approximate formulas. It is now useful to evaluate these errors numerically for typical experimental situations. Such numerical comparisons are one way to directly define the ranges of validity of various approximate formulas and facilitate their uses in reflectivity data analysis. For this purpose, we have selected several SLD profiles to test these approximations. Figure 4 contains four types of density profiles for the surface region of a liquid. Figures 4(a) and 4(b) present a surface SLD profile that starts with a high density value and decreases into a bulk level. Figure 4(a) is a smooth monotonic decay, while Fig. 4(b) oscillates as it goes down. They are both meaningful profiles, as Fig. 4(a) represents a typical exponential adsorption profile on an air-liquid interface and Fig. 4(b) simulates the surface density structure of either a liquid crystal, a microemulsion, a liquid metal, or a polymer film [22–25]. Figures 4(c) and 4(d) show a SLD profile that starts from zero in the air and increases continuously and saturates at the SLD of the bulk liquid. Figure 4(c) is a monotonically increasing SLD, while Fig. 4(d) shows an oscillatory structure as the air-liquid interface is crossed. Figure 4(c) is an error function slope typical of the fussy

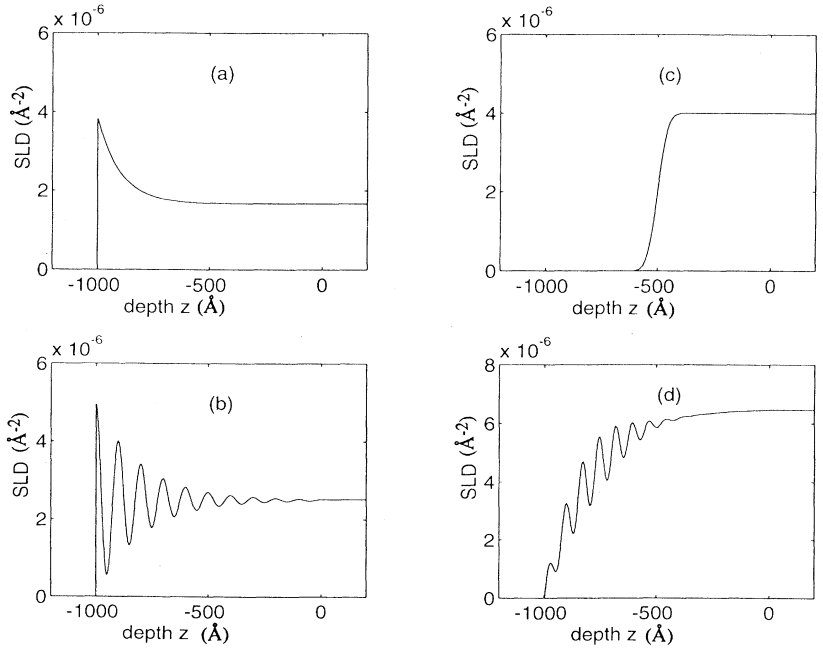

FIG. 4. Four SLD profiles selected for the evaluation of the ranges of validity for various approximate formulas including the WSA, the DWBA, the simplified DWBA, the BA, and the modified BA. All four profiles represent the surface structure of a free liquid. (a) and (b) show a SLD that decreases into the bulk, while (c) and (d) show a SLD that increases into the bulk value.

surface density structure of some simple liquids, and Fig. 4(d) potentially represents a liquid surface that contains an oscillatory density transition from air into the liquid. Altogether, the four profiles in Fig. 4 form a representative set of possible surface structures of free-liquid surfaces. Figure 5 presents four possible profiles of a film on top of a solid substrate. The film in 5(a) or 5(c) has a continuous profile, while that in (b) or (d) has a discrete profile. Furthermore, Fig. 5(a) has a SLD that decreases along the depth, while Fig. 5(c) has a SLD that increases along the depth. The SLD profiles of a film in Figs. 5(b) and 5(d) do not have a general trend of increasing or decreasing as z increases. Therefore, Fig. 5 has included increasing, decreasing, and fluctuating SLD profiles and covers a suitable range for the purpose of evaluating approximate formulas. Figure 5(a) is a typical profile for the diffuse interface of a polymer bilayer on top of a silicon substrate [26]. Figure 5(c) is a typical Gaussian adsorption profile at the interface of a polymer blend and a silicon substrate. Figure 5(b) is typical of the surface structure of an end-functionalized polymer film on a substrate. Figure 5(d) simulates a Langmuir-Blodgett film. In the following, the WSA, the DWBA and the BA will be numerically compared and analyzed. In particular the modified BA in Eq. (56) and the simplified DWBA in Eq. (40) will also be evaluated.

1. BA and the modified BA

We have computed the reflectivities of the SLD profiles in Fig. 4 using Parratt's formula Eq. (1), the BA formula Eq. (47), and the modified BA in Eq. (56) and the results are plotted in Fig. 6. The plots 6(a)–6(d) correspond to the SLD profiles 4(a)–4(d), respectively. The solid lines are based on Parratt's formula, the dashed lines represent the BA results using Eq. (47), and the black circles are the results from the modified Ba result, Eq. (56). We observe that the BA is accurate at large Q for all four profiles. However, as Q becomes smaller, the BA causes significant errors, especially near the critical region, and the BA diverges as Q approaches zero. By forcing the BA to apply to a smooth and sharp surface, the modified BA formula in Eq. (56) has improved the accuracy of the BA significantly, and in particular, has eliminated the divergence at low Q by forcing the reflectivity to be unity at $Q=0$. In Figs. 6(a)–6(c), the modified BA gives very accurate results from the critical edge down to large Q. In Fig. 6(d), the modified BA is not very accurate near the critical edge but is accurate for Q clearly removed from the edge. For practical applications of reflectivity data analysis, we conclude that the modified BA formula Eq. (56) is accurate for data analysis for free-liquid surfaces.

Similar computations are shown in Fig. 7 for the profiles in Fig. 5 with a respective correspondence between the profiles 5(a)–5(d) and the reflectivity curves 7(a)–7(d). The BA results (in dashed lines) again diverge at $Q=0$ and are noticed to be very inaccurate. The modified BA does eliminate the divergence at $Q=0$ but does not improve the accuracy appreciably. Both the BA and the modified BA are not adequate for describing the reflection from films on top of substrates, as seen in Fig. 7, and the cause is the general negligence of the phase effect due to the film SLD. A universal error in all four cases is the shift in phase of the BA or the modified BA results relative to the exact Parratt results. This effect is not obvious in our previous calculations for liquid surfaces because there are no strong reflections deep inside a liquid. In comparison, the film-substrate interface in Fig. 5 causes significant reflection and the reflected wave from the interface has to traverse a thick region of the film to reach the incident space. The film SLD effectively

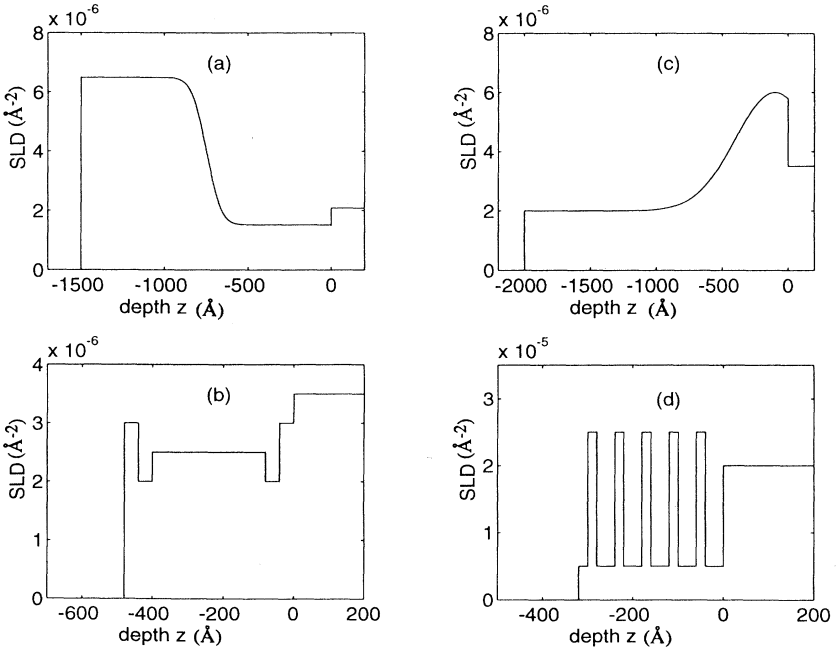

FIG. 5. Four SLD profiles selected for the evaluation of the ranges of validity for various approximate formulas including the WSA, the DWBA, the simplified DWBA, the BA, and the modified BA. All four profiles represent a thin film on top of a substrate. (a) is typical of the diffused interface of a polymer bilayer on top of a silicon substrate, and (c) shows the SLD of the adsorption of polymers onto a solid substrate. (b) is typical of the surface/interface structure of film of end-functionalized polymers. (c) Simulates typical Langmuir-Blodgett films. The high SLD values in (d) signify that the SLD is for x rays.

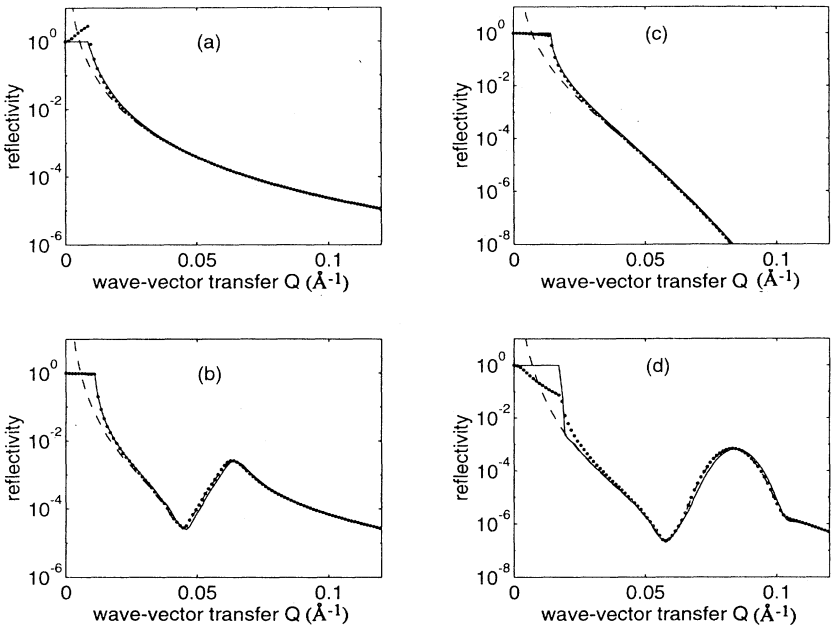

FIG. 6. Comparison between the BA, the modified BA and the exact result using Parratt's formula for the four profiles in Fig. 4. The subfigures (a)–(d) correspond to the subfigures 4(a)–4(d), respectively. The solid lines are the exact Parratt result for the reflectivities. The dashed line is the standard BA result for the reflectivities. The black circles are the reflectivities calculated from the modified BA in Eq. (56).

changes the phase of the wave significantly because the path from the film-substrate interface and the air surface is long enough to make the phase shift appreciable. We also note that both the BA and the modified BA approach the exact result at large Q, so that they are useful if only large-Q data are to be analyzed.

2. *DWBA and the simplified DWBA*

We calculated the reflectivities of the profiles in Fig. 4 using Parratt's formula, the DWBA in Eq. (25), and the simplified DWBA in Eq. (40), and plotted the results in Fig. 8. The Parratt results are in solid lines, the DWBA in dashed lines, and the simplified DWBA in dark circles. The four plots 8(a)–8(d) respectively correspond to the four profiles 4(a)–4(d). We observe that both the DWBA and the simplified DWBA give indistinguishable results for these four profiles and both are fairly accurate. This means, for these liquid surfaces, the simplified DWBA Eq. (40) can be used to replace the more complex regular DWBA formula Eq. (25) without losing accuracy. We also see that the DWBA result in Fig. 8(a) is more accurate than the modified BA result in Fig. 6(a) below the critical point but is less accurate than the modified BA for Q greater than the critical point due to the point that dips down there. In Fig. 8(b), the DWBA shows very

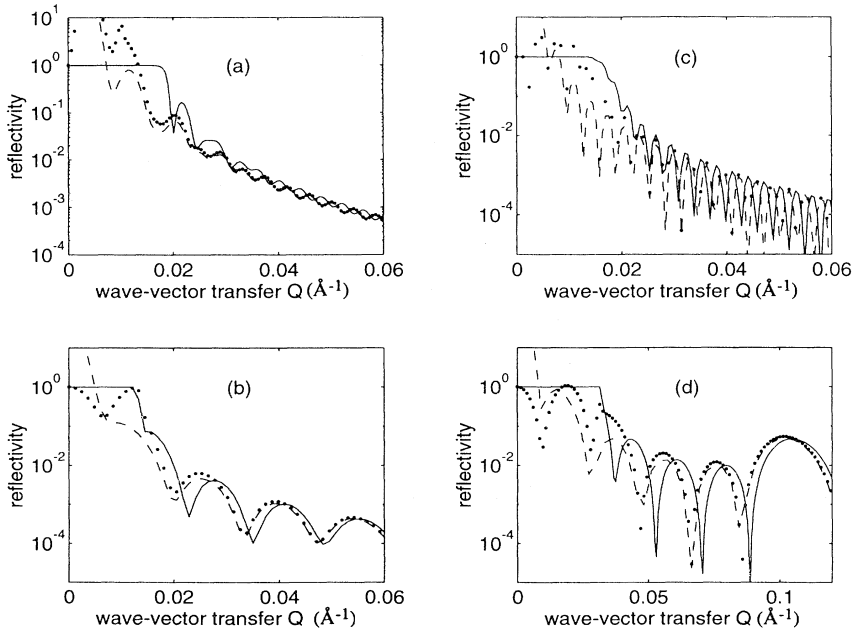

FIG. 7. Comparison of the BA, the modified BA, and the exact result using Parratt's formula for the four profiles in Fig. 5. The subfigures (a)–(d) correspond to the subfigures 5(a)–5(d), respectively. The solid lines are the exact Parratt result for the reflectivities. The dashed line is the standard BA result for the reflectivities. The black circles are the reflectivities calculated from the modified BA in Eq. (56).

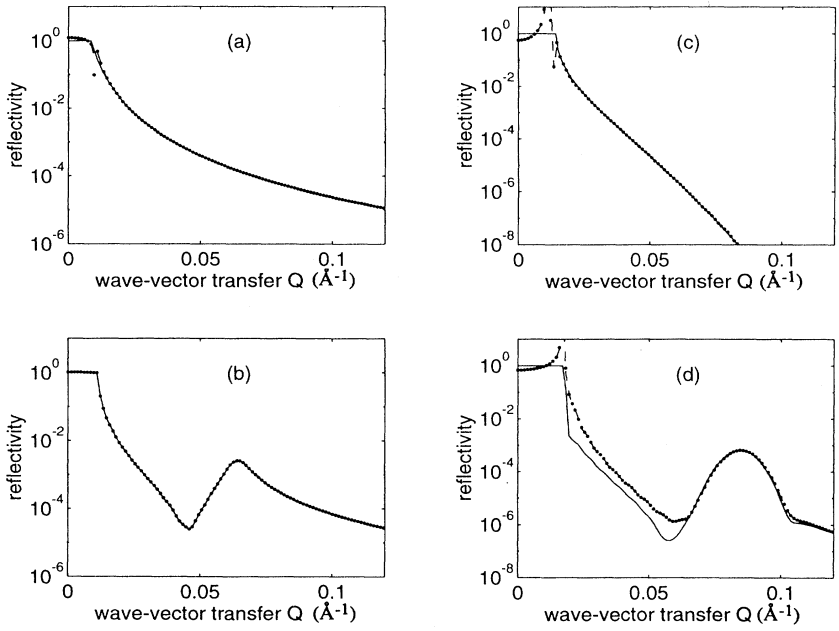

FIG. 8. Comparison of the DWBA, the simplified DWBA, and the exact result using Parratt's formula for the four profiles in Fig. 4. The subfigures (a)–(d) correspond to the subfigures 4(a)–4(d), respectively. The solid lines are the exact Parratt result for the reflectivities. The dashed line is the regular DWBA result Eq. (36) for the reflectivities. The black circles are the reflectivities calculated from the simplified DWBA in Eq. (40). It is seen that the DWBA and the simplified DWBA are indistinguishable in accuracy for these four SLD profiles.

high accuracy over the entire Q range. The modified BA result in Fig. 6(b) is also very accurate in the critical region, but suffers a phase shift around $Q=0.05$ Å^{-1}. For this region, the DWBA is more accurate than the modified BA. The DWBA result in Fig. 8(c) is fairly accurate but is less accurate than the modified BA result in Fig. 6(c) near the critical edge. Lastly, Fig. 8(d) also shows that the DWBA provides a fair fit for $Q>0.06$ Å^{-1} but contains significant errors for $Q<0.06$ Å^{-1}. It is less accurate than the modified BA result in Fig. 6(d). Overall, the DWBA formula (or the simplified DWBA formula) is fairly accurate for liquid surfaces but is not superior to the modified BA formula. As a result, it is recommended that the modified BA formula Eq. (56) be used for data analysis of reflectivities from free-liquid surfaces considering both its accuracy and simplicity of form.

Similar calculations are carried out for the four profiles in Fig. 5. The results are plotted in Fig. 9, with the solid lines denoting the Parratt formula results, the dashed lines the DWBA results and the black circles the simplified DWBA results. We first observe that the simplified DWBA is as accurate as the DWBA for all Q values except around the critical region, where the former is more accurate than the latter. The simplified DWBA reduces the erroneous fluctuation of the

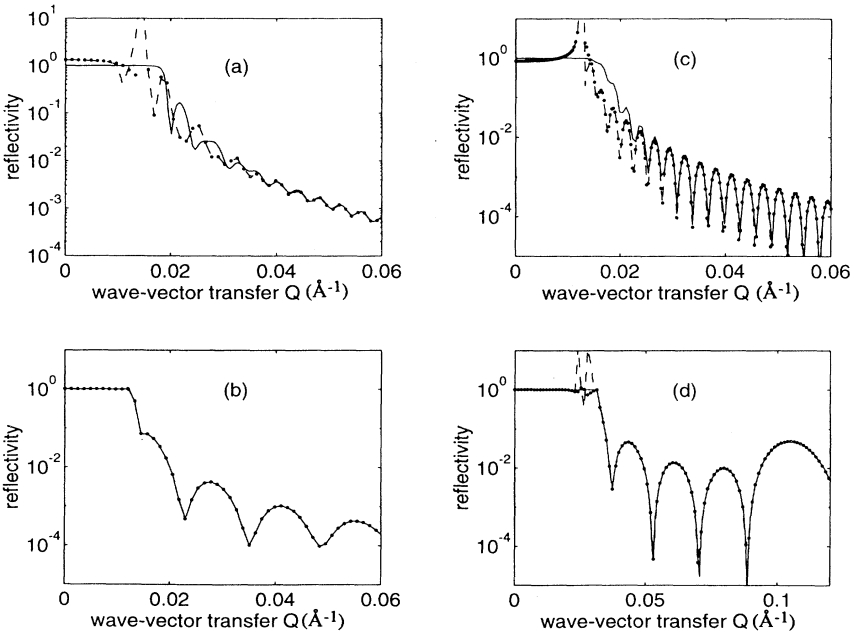

FIG. 9. Comparison of the DWBA, the simplified DWBA, and the exact result using Parratt's formula for the four profiles in Fig. 5. The subfigures (a)–(d) correspond to the subfigures 5(a)–5(d), respectively. The solid lines are the exact Parratt result for the reflectivities. The dashed line is the regular DWBA result Eq. (36) for the reflectivities. The black circles are the reflectivities calculated from the simplified DWBA in Eq. (40). It is seen that the simplified DWBA is more accurate than the regular DWBA on the critical plateau.

reflectivity in the DWBA in the critical region. Combined with the findings in Fig. 8, we conclude that the simplified DWBA is more accurate than the DWBA and should be used owing to both its simpler form and its higher accuracy compared to the regular DWBA. The simplified DWBA is very accurate in Fig. 9(b) with a perfect fit with the exact result, and it is almost a perfect fit in Fig. 9(d), except for a small error right below the edge. In Figs. 9(a) and 9(c), the simplified DWBA is accurate for $Q > 0.02$ Å^{-1}, but is not accurate near the critical edge. Overall, a common feature of all four plots is that the simplified (or the regular) DWBA accounts for the phase of the oscillations in the reflectivities very well in regions other than the vicinity of the critical edge.

In summary, we conclude that the simplified DWBA is simpler and more accurate than the regular DWBA and should be used for surface films on top of substrates, while the modified BA should be used for free-liquid surfaces owing to its simple form and high accuracy.

3. *The WSA, the simplified DWBA and the modified BA*

In Figs. 10(a)–10(d) the reflectivities are plotted for the profiles in Fig. 4 calculated from Parratt's formula (solid lines), the WSA (black circles), and either the modified BA or the simplified DWBA (dot-dashed lines). Similar calculations for the profiles in Fig. 5 are shown in Figs. 11(a)–11(d). In Fig. 10, we compare the WSA result with the modified BA result plotted in dashed lines. Note that the dashed lines are not visible in some portions of the Q range because they coincide with the Parratt result (solid lines). In Fig. 10(a), the WSA is as accurate as the modified BA for Q greater than the critical edge. It is less accurate than the modified BA for a small region right after the edge, but is more accurate than the modified BA for the region below the critical edge. In Fig. 10(b), the WSA is very accurate for $Q > 0.02$ Å^{-1}, while the modified BA suffers a phase shift in this region. However, the WSA does contain approximately 10–20 % errors around the critical edge, as shown in the figure, while the modified BA is very accurate. If the need in data fitting is considered, this comparison puts both the WSA and the modified BA at a comparable level of usefulness. A similar observation can be made from Fig. 10(c) regarding the relative accuracies of the WSA and the modified BA. Finally, Fig. 10(d) shows that the WSA is extremely accurate for Q greater than the critical edge, while the modified BA has bigger errors in the critical region and some errors for $Q > 0.05$ Å^{-1}. From all four figures, 10(a)–10(d), we conclude that the WSA is always very accurate for Q away from the critical edge, whereas the accuracy of the modified BA varies from situation to situation. Thus the WSA is a little superior to the modified BA, although they both sometimes give accurate results.

In Figs. 11(a)–11(d), the WSA is compared with the simplified DWBA results (in dashed lines). Again we see that the WSA is highly accurate for all Q except for the region around the critical edge. The simplified DWBA contains even bigger errors in the same critical region. For example, in Fig. 11(a), the WSA is almost exact except for one point at the critical edge, but the simplified DWBA contain large errors until $Q = 0.03$ Å^{-1}. In Fig. 11(b), the simplified DWBA is very accurate and the WSA is a little less accurate than it is at one point. In Fig. 11(c), it is obvious that the WSA (circles) is more accurate than the simplified DWBA (dashes) right after the critical edge. The WSA is accurate from large Q all the way down to the critical edge, while the simplified DWBA starts to fail when Q falls below 0.02 Å^{-1}. In Fig. 11(d), the simplified DWBA is as accurate as the WSA for $Q > 0.04$ Å^{-1} but is more accurate than the WSA for $Q < 0.04$ Å^{-1}. This is because the profile in Fig. 5(d) is well approximated by an average film plus a

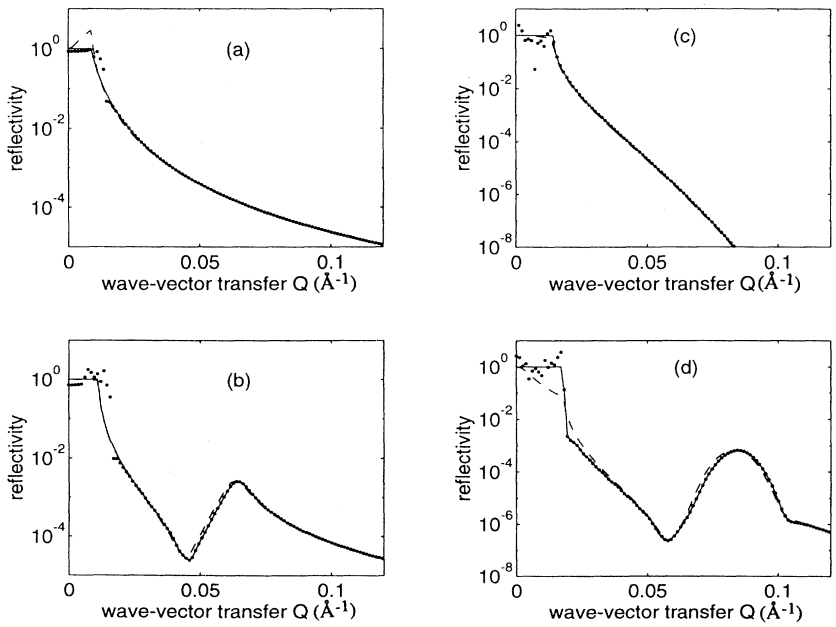

FIG. 10. Comparison of the WSA, the modified BA, and the exact result from Parratt's formula for the four profiles in Fig. 4. The subfigures (a)–(d) correspond to the subfigures 4(a)–4(d), respectively. The solid lines are the exact Parratt result for the reflectivities. The dashed line is the modified BA result Eq. (56) for the reflectivities. The black circles are the reflectivities calculated from the WSA.

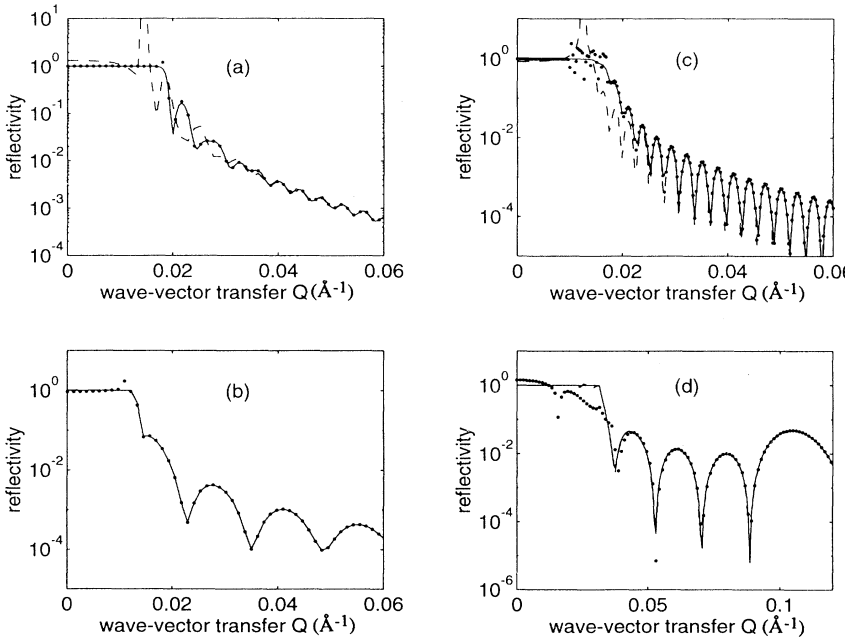

FIG. 11. Comparison of the WSA, the simplified DWBA, and the exact result from Parratt's formula for the four profiles in Fig. 5. The subfigures (a)–(d) correspond to the subfigures 5(a)–5(d), respectively. The solid lines are the exact Parratt result for the reflectivities. The dashed line is the simplified DWBA result Eq. (40) for the reflectivities. The black circles are the reflectivities calculated from the WSA.

deviation. The WSA loses some accuracy because the neglected multiple reflection effect is significant between the many sharp interfaces existing in the profile. However, for the data fitting purpose, both approximations can be used efficaciously considering that both approximations can fit the exact result for almost all oscillation peaks in the figure. In conclusion, the WSA is almost as good as the simplified DWBA and is sometimes better than the simplified DWBA, thus the WSA is recommended for SLD profiles of the types represented by Fig. 5. Note that, for Langmuir-Blodgett films, the simplified DWBA is very useful and should be preferred for data fitting use.

In summary, the WSA can be used for both free-liquid surfaces and films on top of solid substrates, and the accuracy is sufficient for experimental data analysis for the entire region of Q. The modified BA is accurate for free-liquid surfaces and the standard BA formula is only valid for large Q or for very thin surface structure. The standard BA is less accurate than the modified BA for free-liquid surfaces. For films on top of substrates, both the modified BA and the standard BA are inaccurate and cannot be used. For free-liquid surfaces, the simplified DWBA and the regular DWBA give indistinguishable results, but the results are not more accurate than the modified BA results. For films on top of substrates, the simplified DWBA is more accurate than the regular DWBA and both, in turn, are more accurate than the modified BA. Therefore, we recommend either using the WSA for both liquid surfaces and films on substrates or use the modified BA for free liquids plus the simplified DWBA for films on substrates. However, the modified BA and the simplified DWBA may be preferred in specific applications because the WSA may not be the easiest formula to use despite its wide range of validity and higher accuracy. For example, the modified BA may be most efficient for data analysis for free-liquid surfaces and the simplified DWBA may be most convenient and accurate for Langmuir-Blodgett films.

III. NONLINEARITY IN THE REFLECTANCE-SLD RELATIONSHIP

This section analyzes various aspects of nonlinearity in the relationship between the reflectance r and the SLD profile $\rho(z)$. The origin of nonlinearity will be discussed first. Then, a criterion will be established to divide a reflectivity curve into a nonlinear region and a linear region. An analysis will be given regarding how the SLD profile affects different regions and various characteristics of a reflectivity curve, such as the total reflection plateau, oscillation amplitude, and oscillation period.

A. Physical origin of nonlinearity

The origin of nonlinearity can be appreciated by comparing Parratt's formula with the BA which is purely linear. Remember that the BA is obtained in Sec. II D by making several omissions. Each omission corresponds to one source of nonlinearity. The first omission is the second term in the denominator of Parratt's recurrence formula. This term is due to multiple reflections between the interface at $z=z_n$ and the medium beneath $z=z_{n+1}$. Another omission is the effect of ρ_{n+1} on the phase in the exponential term $\exp(2ik_{n+1}\Delta z_{n+1})$. Since $k_{n+1}=(k_0^2-4\pi\rho_{n+1})^{1/2}$, the phase depends on the SLD in a nonlinear fashion. Physically, the interaction of the wave with the medium SLD changes the phase speed of the wave and the change depends on the SLD nonlinearly. Thus the second source of nonlinearity is the dependence of the phase speed on the medium SLD, which is included in the WSA. The third approximation in reaching the BA is Eq. (50), where the nonlinear dependence of the Fresnel reflectance on the SLD is omitted. The actual

dependence should be

$$R_p=\frac{4\pi(\rho_p-\rho_{p-1})}{(k_{p-1}+k_p)^2}\ , \tag{57}$$

which shows that the Fresnel reflectance does not only depend on the step change of the SLD, but also on the magnitude of the SLD relative to k_0^2. In the continuous limit, the denominator in Eq. (57) becomes $4k^2$. The WSA formula obviously has included this part of nonlinearity completely.

B. Determination of the nonlinear region in a reflectivity curve

We use the WSA formula to determine the division point which separates a linear region from a nonlinear region in a reflectivity curve. The phase shift for two wavelets reflected at two locations separated by a distance d^* can be written as

$$\Delta\phi=\left|2\int[k_0-k(z)]dz\right|\ , \tag{58}$$

where the integration is over the medium between the two locations. Such a phase shift will cause a difference in the reflectivity of the film compared to the Born approximation result. The reflectivity of these two interfaces alone can be calculated from the WSA formula as

$$|r_0|^2\approx|R_1|^2+|R_2|^2+2\,\mathrm{Re}[R_1R_2^*]\cos\left[2\int k(z)dz\right]\ , \tag{59}$$

where R_1 and R_2 are the Fresnel reflectances of the two interfaces, respectively. Neglecting the SLD in the phase of the cosine term will cause a relative error in reflectivity given by

$$\frac{\Delta|r_0|^2}{|r_0|^2}\approx\frac{2\,\mathrm{Re}[R_1R_2^*]\left[\cos\left[2\int k(z)dz\right]-\cos\left[2\int k_0dz\right]\right]}{|R_1|^2+|R_2|^2+2\,\mathrm{Re}[R_1R_2^*]\cos\left[2\int k(z)dz\right]}\ . \tag{60}$$

As the third term in the denominator is always less than the sum of the first two terms, the relative change of the reflectivity has an upper limit

$$\frac{\Delta|r_0|^2}{|r_0|^2}\le\frac{1}{2}\left|\cos\left[2\int k(z)dz\right]-\cos\left[2\int k_0dz\right]\right|\le\frac{\Delta\phi}{2}\ . \tag{61}$$

For this error to be small, we demand it be less than a value τ to obtain

$$Q_0=\frac{4\pi}{\tau}|\bar{\rho}^*d^*|\ , \tag{62}$$

$$\bar{\rho}^*\equiv\frac{1}{d^*}\int\rho\,dz\ , \tag{63}$$

where d^* is the thickness of the structural region of the film and $\bar{\rho}^*$ is the average SLD in this region. For a free-liquid surface, d^* can be calculated by locating the region in which the slope of the SLD is no less than $\sqrt{\tau}$ times the maximum slope of the SLD in the entire surface. For a film on top of a substrate, $d^*=d$ and $\bar{\rho}^*=\bar{\rho}$, the average SLD in the whole film. In an experiment, if the approximate thickness and average SLD $\bar{\rho}$ are known, one can estimate the regions of linear and nonlinear reflectivities by Eq. (62).

C. Nonlinear effect on amplitude, phase, and total reflection of reflectivity curve

The difference between the WSA and the BA lies in the amplitude and the propagation factor. In the amplitude, the linear BA contains at term $1/k_0^2$, while the WSA contains $1/k^2$. If everything else is equal, then the amplitude of the WSA is larger than that of the BA because $k<k_0$ for positive SLD $\rho(z)$, which is true for most materials, i.e.,

$$\frac{\pi}{k^2}\ge\frac{\pi}{k_0^2}\quad\text{for }\rho\ge0\ , \tag{64}$$

$$\frac{\pi}{k^2}\le\frac{\pi}{k_0^2}\quad\text{for }\rho\le0\ , \tag{65}$$

$$\frac{\pi}{k_1^2}\le\frac{\pi}{k_2^2}\quad\text{for }\rho_1\le\rho_2\ . \tag{66}$$

Equation (64) states that the amplitude is higher than the Born approximation for positive SLD and Eq. (65) says that it is smaller than the BA for negative SLD. Equation (66) states that if the SLD increases from ρ_1 to ρ_2, the amplitude increases accordingly.

In the exponential propagation factor in Eq. (9), the phase is an integral of $2k$. In the linear BA in Eq. (54), the phase is an integral of $2k_0$. For positive SLD, $k<k_0$ so that the actual wave according to the WSA lags in phase behind the BA approximate wave. For negative SLD, the actual wave gains in phase (i.e., phase advance) compared to the BA approximate wave. In summary, we find

$$2\int_{-d}^{z}k(z)dz<2k_0(z+d)\ , \tag{67}$$

a phase lag for $\rho>0$,

$$2\int_{-d}^{z}k(z)dz>2k_0(z+d)\ , \tag{68}$$

a phase advance for $\rho<0$. When $k(z)$ becomes imaginary for positive SLD, the exponential term in the WSA becomes

$$A = \exp\left[2i\int_{-d}^{z} k(z)dz\right] = \exp\left[-2\int_{-d}^{z}\sqrt{4\pi\rho - k_0^2}\,dz\right], \quad (69)$$

which is now an attenuation factor. The larger the z, the smaller the value of the factor. It represents an evanescent wave which decays into the surface film. When k_0^2 is much smaller than $4\pi\rho$, the exponential term becomes negligible. As a result, only one term in the WSA is significant, which is the Fresnel reflectance due to the front surface at $z=-d$, at which the exponential term in Eq. (9) becomes one. Since the modulus of the Fresnel reflectance becomes unity when k becomes imaginary, the reflectivity calculated from the WSA becomes unity, corresponding to total reflection.

IV. CONCLUSION

A comprehensive analysis is given about the functional relationship between neutron or x-ray reflectance and the scattering-length-density profile of a surface film. Derivations are presented to obtain the differential equation for the reflectance, the WSA, the DWBA, and the BA from Parratt's formula. Such derivations have unified existing reflection theories under Parratt's formula. In particular, the derivations have revealed that the differential equation is the continuous counterpart of Parratt's formula, the WSA is an approximation that neglects the multiple reflection effect but retains the dependence of the phase speed and the Fresnel reflectance on the film SLD, the DWBA approximates multiple reflections and the SLD dependence of the phase speed and Fresnel reflectance with those inside an average film, and the BA neglects all of multiple reflections and the SLD dependence of the phase speed and the Fresnel reflectance. A simplified DWBA formula, Eq. (40), is derived from the WSA and shown to be simpler and more accurate than the regular DWBA.

Numerical analysis was carried out for a range of SLD profiles to evaluate the validity and utility of various approximations. It was found that the BA is accurate only for large Q for all SLD profiles. For free-liquid surfaces, the modified BA is demonstrated to be very accurate and is highly recommended for its simple form. For films on top of substrates, the modified BA is very inaccurate. The DWBA result is in general accurate for liquid surfaces, too, but is less good than the modified BA. However, it is fairly accurate for films on top of solid substrates. However, the simplified DWBA Eq. (40) was shown to be even simpler yet more accurate than the regular DWBA near the critical region, thus it can be used to replace the regular DWBA. The WSA is found to be valid for both free-liquid surfaces and films on top of substrates, covering the ranges of validity of both the modified BA and the simplified DWBA. However, the WSA may not always be the easiest to use for certain applications. For instance, the modified BA is very simple and very accurate for the thin surface region of a simple liquid and may be preferred to the WSA. Another example is Langmuir-Blodgett films, for which the simplified DWBA is even more accurate than the WSA near the critical region and may be preferred. However, for analyzing the functional relationship between the SLD profile and the reflectivity curve either to gain understanding or to develop or improve model-independent methods for data inversion, it is much more convenient to use the WSA. For example, the phase and amplitude effect of nonlinearity on a reflectivity curve as discussed in Sec. III is most conveniently studied through the WSA formula.

Based on the above derivations and understanding, the nonlinearity in the reflectance-SLD relationship is analyzed systematically. It is determined that the nonlinearity comes from three sources: multiple reflections, the nonlinear dependence of the Fresnel reflectance on the SLD, and the dependence of the phase speed on the SLD. It found that the effect of nonlinearity on reflectivity decreases as Q increases because the film SLD ρ influences reflection through $k=(k_0^2-4\pi\rho)^{1/2}$ with $k_0=Q/2$. This suggests that nonlinearity may be negligible when Q becomes sufficiently large. To determine how large Q has to be for nonlinearity to be negligible, a dividing point Q_0 is quantitatively obtained in Eq. (62). In the linear region $Q>Q_0$, the BA is valid approximately with error less than τ. In the nonlinear region $Q<Q_0$, the BA contains errors greater than τ and cannot be used.

In the nonlinear region, the nonlinear effect changes the amplitude of a reflectivity curve such that a larger SLD usually corresponds to a higher amplitude in the reflectivity curve. It affects the phase of a reflectivity curve such that, compared to the BA result, a positive SLD causes a phase lag while a negative SLD causes a phase advance in a reflectivity curve. Numerical calculations were carried out and confirmed the above observations. It was also found that the exponential phase factor in the WSA accounts for evanescence and total reflection when k becomes imaginary. The results obtained in this paper may be useful for developing new methods or improving existing methods for reflectivity data analysis.

ACKNOWLEDGMENTS

This work was supported by the Massachusetts Institute of Technology Sloan Funds. The author would like to acknowledge insightful discussions with Professor S.-H. Chen.

[1] G. P. Felcher and T. P. Russell, Phys. B **173**, 1 (1991).
[2] D. S. Sivia, W. A. Hamilton, and G. S. Smith, Phys. B **173**, 121 (1991).
[3] B. E. Warren, *X-Ray Diffraction* (Addison-Wesley, Reading, MA, 1969).
[4] X.-L. Zhou and S.-H. Chen, Phys. Rev. E **47**, 3174 (1993).
[5] X.-L. Zhou, G. P. Felcher, and S.-H. Chen, Phys. B **173**, 167 (1991).
[6] X.-L. Zhou, S.-H. Chen, and G. P. Felcher, J. Phys. Chem. **95**, 9025 (1991).

[7] X.-L. Zhou, S.-H. Chen, and G. P. Felcher, Phys. Rev. A **46**, 1839 (1991).
[8] J. Als-Nielsen, Z. Phys. Condens. Matter B **61**, 411 (1985).
[9] P. S. Pershan and J. Als-Nielsen, Phys. Rev. Lett. **52**, 759 (1984).
[10] J. Penfold and R. K. Thomas, J. Phys. Condens. Matter **2**, 1369 (1990).
[11] J. Lekner, *Theory of Reflection* (Nijhoff, Boston, 1987).
[12] T. Russell, Mater. Sci. Rep. **5**, 171 (1990).
[13] G. H. Vineyard, Phys. Rev. B **26**, 4146 (1982).
[14] S.-H. Chen, X.-L. Zhou, and B. L. Carvalho, Progr. Colloid Polym. Sci. **93**, 85 (1993).
[15] S. K. Sinha, E. B. Sirota, S. Garoff, and H. Stanley, Phys. Rev. B **38**, 2297 (1988).
[16] M. K. Sanyal, S. K. Sinha, A. Gibaud, K. Huang, B. Carvalho, M. Rafailovich, J. Sokolov, X. Zhao, and W. Zhao, Europhys. Lett. **21**, 691 (1993).
[17] V. F. Sears, Phys. Rev. B **48**, 477 (1993).
[18] X.-L. Zhou and L. He, Phys. Rev. E **49**, 5345 (1994).
[19] L. G. Parratt, Phys. Rev. **95**, 359 (1954).
[20] X.-L. Zhou and S.-H. Chen, Phys. Rep. (to be published).
[21] J. Jacobsson, in *Progress in Optics,* edited by E. Wolf (North-Holland, Amsterdam, 1966), pp. 249–259.
[22] X.-L. Zhou, L.-T. Lee, S.-H. Chen, and R. Strey, Phys. Rev. A **46**, 6479 (1992).
[23] K. A. Dawson, Phys. Rev. A **35**, 1766 (1987).
[24] G. Swislow, D. Schwartz, B. M. Ocko, P. S. Pershan and J. D. Litster, Phys. Rev. A **43**, 6815 (1991).
[25] A. Menelle, T. P. Russell, and S. H. Anastasiadis, Phys. Rev. Lett. **68**, 67 (1992).
[26] G. P. Felcher, A. Karim, and T. P. Russell, J. Non-Cryst. Solids **131**, 703 (1991).